Evidence for impact ionization in vanadium dioxide

Joshua Holleman, Michael M. Bishop, Carlos Garcia, J. S. R. Vellore Winfred, Shinbuhm Lee, Ho Nyung Lee, Christianne Beekman, Efstratios Manousakis, and Stephen A. McGill

Phys. Rev. B **94**, 155129 — Published 17 October 2016

DOI: 10.1103/PhysRevB.94.155129

Evidence for Impact Ionization in Vanadium Dioxide

Joshua Holleman,[1,2] Michael M. Bishop,[1] Carlos Garcia,[1,2] J. S. R. Vellore Winfred,[1] Shinbuhm Lee,[3] Ho Nyung Lee,[3] Christianne Beekman,[1,2] Efstratios Manousakis,[1,2] and Stephen A. McGill[1,*]

[1] *National High Magnetic Field Laboratory, 1800 E. Paul Dirac Dr., Tallahassee, FL 32310*
[2] *Department of Physics, Florida State University, Tallahassee, FL 32306*
[3] *Materials Science and Technology Division, Oak Ridge National Laboratory, Oak Ridge, TN, USA*

(Dated: September 20, 2016)

Pump-probe optical spectroscopy was used to investigate proposed charge carrier multiplication via impact ionization in the M_1 insulating phase of VO_2. By comparing the transient reflectivities of the film when pumped at less than and then more than twice the bandgap energy, we observed a larger ultrafast response with the higher energy pump color while the film was still transiently in the insulating phase. We additionally identified multiple timescales within the charge dynamics and analyzed how these changed when the pump and probe wavelengths were varied. This experiment provided evidence that a fast carrier multiplication process, i.e. impact ionization, acts efficiently in this prototypical strongly-correlated insulator, as was recently predicted by theoretical calculations.

I. INTRODUCTION

Strong electron correlations are the source of novel electronic phases and emergent phenomena that continue to fuel scientific excitement over transition metal oxides[1] and oxide heterostructure interfaces.[2,3] Advances in the fabrication of these complex systems have made it possible to envision devices exploiting such exotic phenomena as multiferroicity, superconductivity, and colossal magnetoresistance. Strong correlations, especially in narrow-gap insulators, also may greatly enhance the rate of impact ionization,[4,5] which is a fast, hot-carrier relaxation pathway in which the absorption of a single photon above an energy threshold excites multiple charge carriers. Here, we provide evidence of impact ionization for the first time in a prototypical strongly-correlated insulator (SCI), vanadium dioxide, using optical transient reflectivity spectroscopy. This observation leads to a deeper understanding of the charge excitation dynamics in SCIs and opens the door to further investigating whether devices based on these materials could lead to a new generation of clean energy technologies. These results will also further broaden interest in SCIs to explore the novel properties strong electron correlations may enable in devices utilizing photoexcited charge.

Vanadium dioxide, VO_2, has received much attention for fundamental research since it has characteristics of both Mott and Peierls insulators[6] as well as an insulator-metal (I-M) transition at about 50 K above room temperature. The fact that this I-M transition can be photo-induced has made VO_2 the subject of a number of pump-probe optical studies.[7–23] In these studies the mechanisms and details of the photoinduced I-M transition have been investigated and various scenarios of the dynamics of the transition under different excitation conditions have been discussed. The aim of the present paper is not to confront any of these interpretations. It is rather to examine evidence for carrier multiplication which may have occurred at a less than 100 fs timescale. While our laser pulses cannot probe this regime directly, a careful analysis of our data can yield evidence for the effects of carrier multiplication at longer time scales. Our interest concerns what happens when, under a low fluence pump, the sample, or parts of it, is in the insulating phase where the

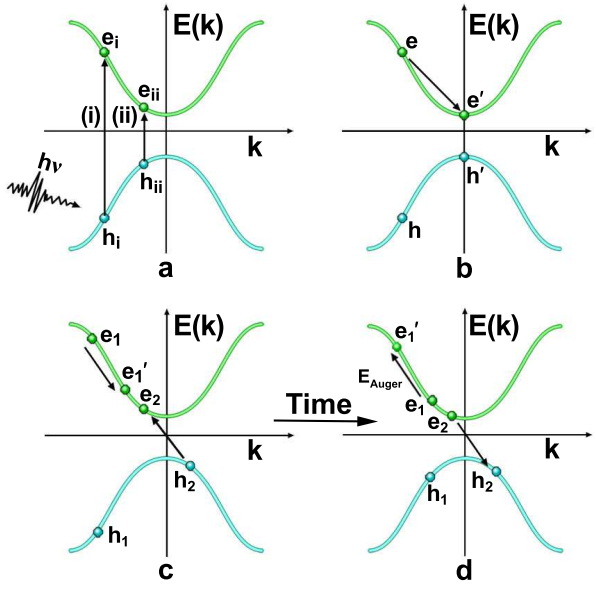

FIG. 1. (a) An incident solar photon promotes an electron from the occupied band to the conduction band (i) with an energy greater than twice the band gap or (ii) near the band edge, creating an electron/hole pair in either case. (b) In a typical conventional insulator, the electron/hole pair dissipates its excess energy beyond the gap via phonon scattering or phonon emission and relaxes to the band edge within a timescale of the order of 0.1 to 1 ps. (c) In the case of a strongly correlated insulator with incident photo-excitation energy greater than twice the band gap (part (a), case (i)), the electron, the hole, or both can give up their excess energy to promote one or more electrons from the valence band to the conduction band through their interaction with the electrons of the occupied bands. (d) Auger recombination is the reverse of impact ionization.

meaning of carrier multiplication through impact ionization makes sense. Therefore, we undertook a fundamentally different study of non-equilibrium charge dynamics in VO_2, not out of interest in the I-M transition, but rather to assess whether photons with energies in excess of twice the bandgap in VO_2 can excite multiple charge carriers on short timescales while VO_2 is still insulating. By exciting a thin film with two different pump wavelengths, one above and one below the expected impact ionization threshold, we observed changes in the amplitude and decay timescale of the transient reflectivity near the conduction band-edge that demonstrated a charge carrier enhancement for the case of the above-threshold pump wavelength. This observation represents the first evidence that a photon can excite multiple electron/hole pairs in an SCI via impact ionization.

A schematic representation of impact ionization is shown in Fig. 1. In this process, an electron from the valence band is promoted to the conduction band via photoexcitation, leaving a hole in the valence band. If the photon energy is significantly larger than the bandgap, the incident photon can promote the electron either from a deeply seated state in the valence band to the conduction band, or from the upper valence band to a highly excited state of the conduction band. In a conventional semiconductor (See Figs. 1a, 1b) the excess energy of the electron/hole pair is dissipated into phonons within a timescale that depends on the material (on the order of 10^{-13}-10^{-12} secs), followed by subsequent relaxation of the electron/hole pair to the band-edge.[24] In the case of an SCI, the strong Coulomb interaction between the highly photo-excited electron or hole and the other electrons occupying valence band states leads to the promotion of another electron from the occupied states to the conduction band by transferring part of its excess energy, as shown in Fig. 1c.[4,5] Finally, electron/hole pairs created via impact ionization can undergo Auger recombination (See Fig. 1d), which is the reverse process to impact ionization.

While the identification of VO_2 as a Mott-insulator is still somewhat unsettled, VO_2 remains an excellent candidate for a proof-of-concept demonstration of impact ionization since the M_1 phase of VO_2 is a prototypical SCI and theoretical calculations indicate fast impact ionization rates (IIR) occur in this material. Some have suggested that VO_2 is a Peierls insulator,[6] namely that the gap opens due to a zig-zag distortion along the rutile axis.[25] Even so, it has been shown that the opening of the Peierls gap is assisted by on-site Coulomb correlations.[6] The IIR of the M_1 phase of VO_2 was computed from first principles,[5] and within the region of the solar spectrum the IIR is more than two orders of magnitude faster in VO_2 than in Si, depending on the energy of the photoexcited electron or hole. Furthermore, the IIR in VO_2 is an order of magnitude higher than its corresponding phonon decay rate. In Ref. 5, it was demonstrated that the high impact ionization rate of VO_2 was associated with the flat d-bands of nearly localized electrons. Vanadium dioxide is the only material that is both broadly agreed to be an SCI and whose impact ionization rate has been so well characterized theoretically. As such it was the best choice for observing an enhanced IIR in a strongly-correlated system.

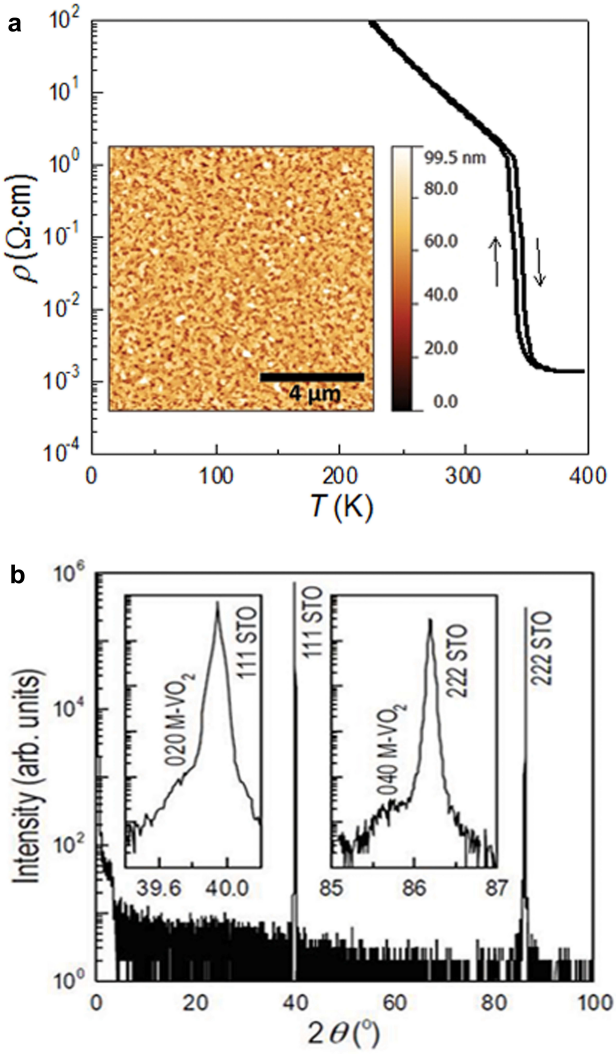

FIG. 2. (a) Resistance vs temperature curve of the VO_2 film. The curve was measured while cooling and heating showing (arrows) slight hysteresis at the metal-insulator transition (T = 345 K). Inset: Atomic force microscope image of the 100 nm VO_2 film grown on (111) $SrTiO_3$ substrate. The scale bar is 4 μm, and the scan size is 10 x 10 μm. (b) θ-2θ scan of a VO_2 film. The insets show enlarged regions around the 111 and 222 $SrTiO_3$ peaks.

II. SAMPLE PREPARATION AND CHARACTERIZATION

We performed our measurements on a 100 nm VO_2 film grown onto a (111) $SrTiO_3$ substrate by pulsed laser deposition. A VO_2 sintered pellet was ablated using a

KrF excimer laser at a wavelength of 248 nm with a laser fluence of about 1 J/cm^2. The growth temperature was 600°C with an oxygen pressure during growth of 25 mTorr.[26,27] After growth, the film's topography was characterized using a MFP-3D atomic force microscope system from Asylum Research. DC transport properties were characterized using a physical properties measurement system (Quantum Design) and structural characterization was done using a four circle x-ray diffractometer (XRD) using Cu-Kα_1 radiation. The transport properties shown in Fig. 2a display the typical resistance vs. temperature behavior for VO_2, namely that the film is insulating at room temperature with an I-M transition (accompanied by the monoclinic to rutile structural transition) observed around T = 345 K. The topography, in Fig. 2a inset, shows an RMS roughness of about 8 nm. Figure 2b shows an XRD θ-2θ scan of the 100 nm VO_2 film. In the XRD data, the film peaks are somewhat obscured by the very strong $SrTiO_3$ peaks due to similar lattice parameters. The insets show enlarged regions around the substrate peaks which clearly indicate the presence of the 020 and 040 VO_2 peaks. No other peaks are observed, showing that the film is pure VO_2 without the coexistence of parasitic oxide phases (such as V_2O_3 and V_2O_5). The XRD data show that the film has the typical monoclinic room temperature structure expected for VO_2.

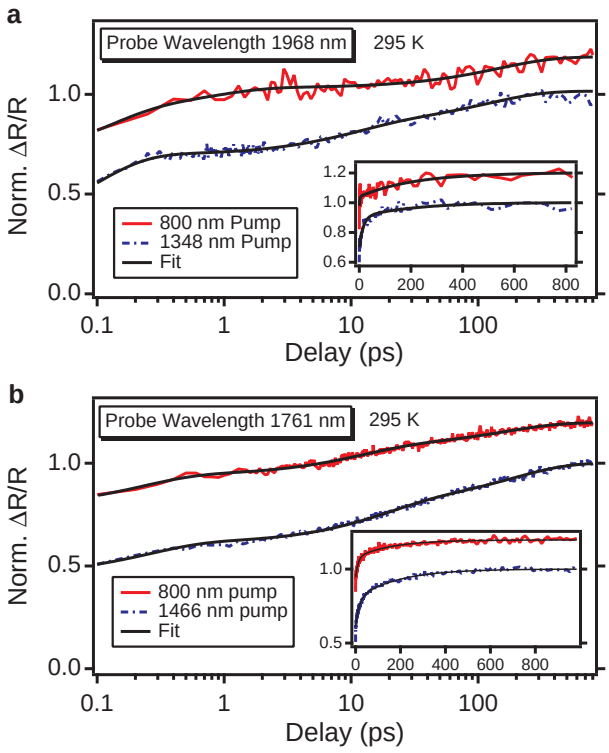

FIG. 3. Normalized VO_2 transient reflectivities. (a) The relative reflectivity change for the 1968 nm probe. (b) The relative reflectivity change for the 1761 nm probe. The 800 nm pump data is offset by 0.2 for clarity in both (a) and (b). Insets contain the same data as their respective panels plotted on a linear time axis.

III. PUMP-PROBE OPTICAL MEASUREMENTS

Pump-probe optical spectroscopy was used to measure the transient reflectivity of a 100 nm VO_2 film. These measurements were accomplished using a 1 kHz regeneratively amplified Ti:Sapphire laser cavity producing 120 fs pulses at 800 nm. This laser was used to pump a TOPAS optical parametric amplifier in order to achieve the near-infrared pump and probe wavelengths that were closer to the energy gap of VO_2 (0.6 eV). We measured the reflectivity at two different probe wavelengths (i.e. 1968 nm [0.63 eV] and 1761 nm [0.70 eV]) in each case varying the excitation (pump) wavelength from below twice the energy gap to above twice the energy gap, keeping the incident fluence fixed for comparisons at the same probe wavelength. The pump wavelengths used were 1348 nm [0.92 eV] (1968 nm probe), 1466 nm [0.85 eV] (1761 nm probe), and 800 nm [1.55 eV] (used with both probe wavelengths). The pump and probe beams were focused to 300 μm diameter spots. The pump pulse energy density was varied from 0.85 mJ/cm^2 to 5 mJ/cm^2 and the probe fluence was less than 100 mW/cm^2 in all cases. The linearly polarized pump and probe beams were overlapped, cross-polarized, and randomly oriented in the plane of the film. The reflected probe intensity was measured using a cooled extended range InGaAs photodiode, and the time-resolved data were collected using standard lockin techniques. All insulating state optical data were collected at room temperature.

The measured reflectivity transients exhibited three timescales in either case of pumping below (1348 nm and 1466 nm) or above (800 nm) the expected impact ionization threshold (i.e. twice the bandgap), and only the intermediate timescale changed significantly with pump wavelength. Figures 3a and 3b report the normalized transient reflectivities for the probe wavelengths of 1968 nm and 1761 nm, respectively. The three timescales in Fig. 3 were obtained by fitting the transients to a sum of increasing exponentials. The results of this fitting with 95% confidence intervals are summarized in Table I. The shortest timescale, τ_1, describes the nearly instantaneous rise of the signal, corresponding to electronic excitation, that completes essentially within the pump-probe overlap. Sample dynamics within the duration of the pulse overlap cannot be resolved. The longest timescale, τ_3, describes the slow rise of the reflectivity to its maximum value, which corresponds to thermal equilibration between the lattice and hot phonons and occurs over 100-200 ps.[9,17] Photo-excitation is thought to preferentially stimulate 6 THz vibrational modes,[10,12,14] which have a lifetime of 100-200 ps.[15,28] Over this timescale, which most closely corresponds in our data to τ_3, the rest of the lattice thermalizes with the photo-stimulated phonon

population.

TABLE I. Transient Reflectivity Rise Times

Pump [nm (eV)]	Probe	τ_1 [ps]	τ_2 [ps]	τ_3 [ps]
800 (1.55) $>$ 2E$_g$	1761 (0.70)	0.22 ± 0.10	11.4 ± 1.4	163 ± 25
1466 (0.85) $<$ 2E$_g$	1761 (0.70)	0.25 ± 0.16	17.0 ± 1.3	188 ± 16
800 (1.55) $>$ 2E$_g$	1968 (0.63)	0.11 ± 0.32	0.8 ± 1.1	146 ± 59
1348 (0.92) $<$ 2E$_g$	1968 (0.63)	0.09 ± 0.01	10.1 ± 3.6	119 ± 79

The intermediate timescale, τ_2, was consistently shorter when pumping with 800 nm (above $2E_g$) than when pumping with the longer pump wavelengths (below $2E_g$) for comparisons at a fixed probe wavelength. This timescale, τ_2, likely corresponds to hot phonon diffusion in the film.[17] Nonetheless, this rate can be accelerated above the limit for ballistic phonon transport through the presence of additional charge carriers stimulated by a faster process. Hence, the shortening of τ_2 could be accomplished by a carrier enhancement via impact ionization when the higher energy pump is used.

Beyond the reduction in τ_2, Fig. 3 further reveals that the fractional contribution to the amplitude of $\Delta R/R$ increased for the fastest component of the transient when using the 800 nm pump. This means that the charge population excited using 800 nm accounted for a larger fraction of the total change in reflectivity than for either of the longer wavelength pumps. This increase is well-illustrated in Fig. 4, which displays the ratio of the reflectivity transients in Fig. 3. The ratios of the normalized transients in Fig. 4a provide estimates of the maximum reflectivity change, which are 1.20 ± 0.03 (1761 nm) and 1.17 ± 0.03 (1968 nm), for the case in which the amplitudes of $\Delta R/R$ are equal. These ratios and the 95% confidence intervals were determined by fitting with double (1761 nm probe) and single (1968 nm probe) exponential decays. Therefore, the 800 nm pump produced an increase in the size of the ultrafast component of $\Delta R/R$, corresponding to a larger photo-excited carrier density.

The reduction of τ_2 and the increase in the fractional amplitude of the τ_1 component caused by the 800 nm pump indicate an enhancement of the photo-excited carrier population over that created by both longer wavelengths. Our $\Delta R/R$ measurements revealed three subprocesses consisting of (from fastest to slowest) electronic excitation (τ_1), hot phonon diffusion (τ_2), and thermal equilibration between the lattice and hot phonons (τ_3). These measurements confirm that the nearly instantaneous response in $\Delta R/R$ is larger for 800 nm photons than it is for the lower energy pump photons.

The dynamics measured in ultrafast optical measurements are often conceptually understood using a two-temperature model[29] where the optical energy is first imparted to the charge carriers, which then thermalize with the lattice and warm it. In the case of VO_2, lattice heating due to the thermalization of hot carriers occurs on a timescale of 100 fs to 1 ps.[11,24] The amount

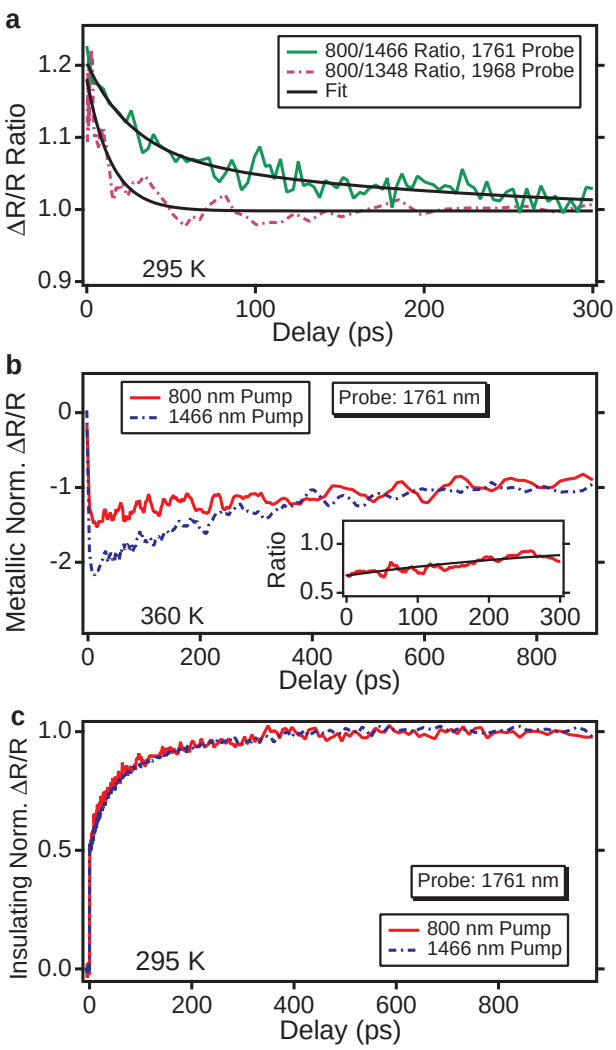

FIG. 4. VO_2 transient reflectivity ratios and metallic state comparison. (a) The ratios of the transient reflectivities for both sets of data in Fig. 3. (b) The normalized transient reflectivities in the metallic state. The sign of the reflectivity is inverted from the insulating phase. Inset: The 800/1466 pump ratio of the normalized data in (b). The data in (a) and (b) were smoothed using moving averages. (c) Normalized transient reflectivities in the insulating state taken at 2.6 mJ/cm^2 for the 1466 nm pump and 1.45 mJ/cm^2 for the 800 nm pump.

of lattice heating can also be expected to increase with the use of more energetic photons, which might also contribute to an increased dynamical response. With our laser pulses, we are not able to observe the characteristic times for dynamics that occur in less than 100 fs. However, based on the results of ab initio calculations,[5] and even on more general grounds,[4] we expect that on an approximate timescale of 10 fs, impact ionization will act as a carrier multiplication process, provided that the photoexcited electron or hole has sufficient energy beyond the gap. Therefore, guided by this theoretical work, we looked for evidence of impact ionization in ultrafast op-

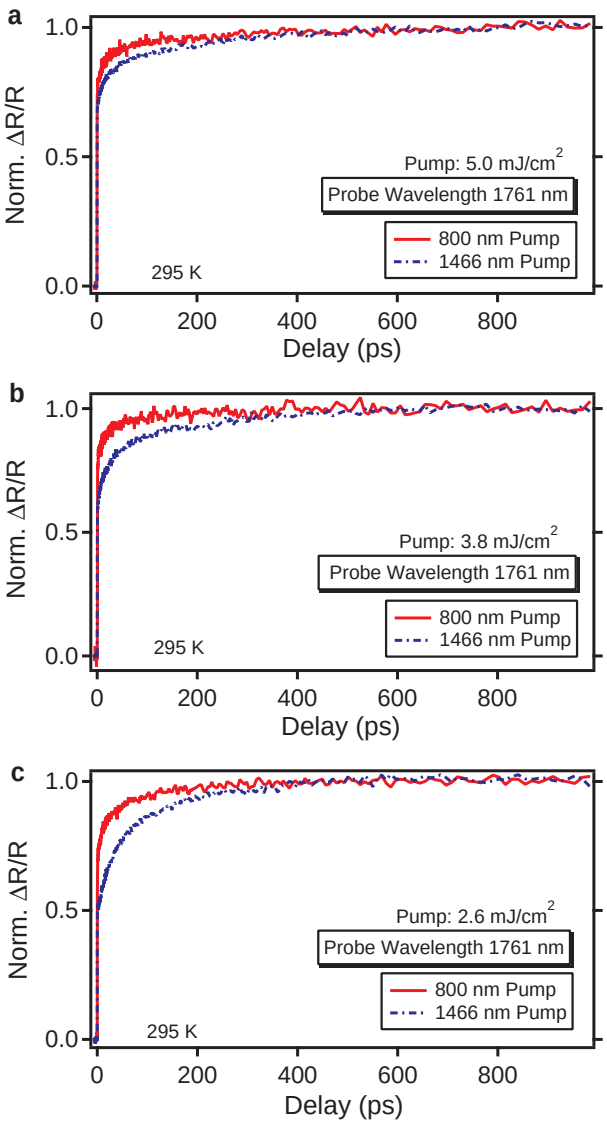

FIG. 5. (a)-(c) The normalized transient reflectivities taken with pump energy densities of 5.0 mJ/cm^2, 3.8 mJ/cm^2, and 2.6 mJ/cm^2, respectively.

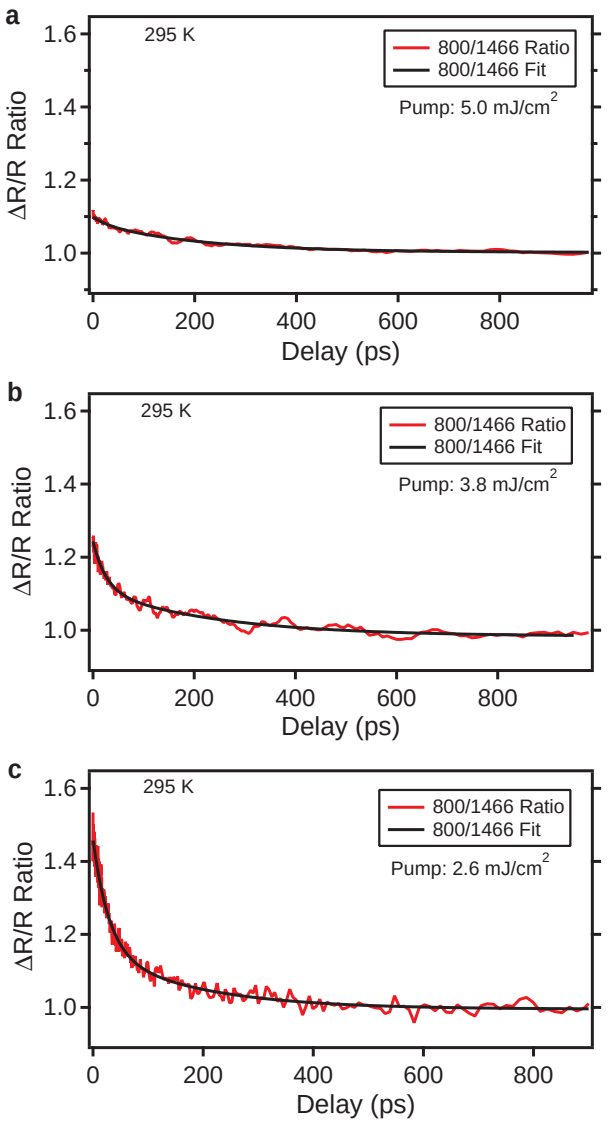

FIG. 6. (a)-(c) The 800/1466 ratios of the transients shown in Fig. 5, respectively. The data in (a) and (b), but not (c) were smoothed using moving averages.

tical reflectivity measurements.

IV. OPTICAL PENETRATION DEPTH ANALYSIS

Analysis of the penetration depths in VO_2 indicated that similar numbers of photons should be absorbed at each pump color when similar incident pump energy densities were used. Using the results of Verleur, *et al.*,[30] we obtained the real and imaginary parts of the dielectric constant for a 100 nm film of VO_2. Using these values, the refractive indices and penetration depths for the various pump wavelengths were calculated. We used the expression for the penetration depth, d: $d = \lambda/4\pi\kappa$, of the light intensity for our calculations, where lambda was the wavelength and kappa was the extinction coefficient. The penetration depth for the probe and each pump wavelength in the insulating state was more than 100 nm. The results of this analysis revealed that approximately 48% of the 800 nm pump and 26% of the 1466 nm pump were absorbed in the 100 nm depth of the film. Since the ratio (1466/800) of incident pump photons was 1.83, the film absorbed roughly the same number of photons at each pump color. This was similarly true for the 1348 nm pump. We also did not observe significant differences in the reflection losses from the film. As a result, though we consistently use the incident pump energy density (mJ/cm^2) to label the transient reflectivity comparisons made in this discussion, the analysis does

take into account the expected total number of absorbed photons within the film depth and therefore considers the total absorbed energy density (mJ/cm^3) as the important parameter of the excitation.

We repeated the 800/1466 transient reflectivity comparison at 360 K and found that the reflectivity enhancement did not occur in the metallic phase. The transient reflectivities measured with the 1761 nm probe are shown in Fig. 4b where the signals at long delay have been normalized to −1 because the sign of the response was inverted in the metallic phase. Re-analysis of the penetration depths for the metallic state[30] indicated that the probe wavelength had a penetration depth shorter than either pump beam, about 50 nm. With these changes caused by the phase transition, approximately half as many 800 nm photons were absorbed as 1466 nm photons in the metallic state. The 1466 nm pump in Fig. 4b produced a larger response than the 800 nm pump near zero delay. The inset shows the 800/1466 nm ratio, which was 0.67 ± 0.03. For comparison, we performed a similar test in the insulating phase (Fig. 4c) to approximate the absorbed energy densities in the metallic conditions where less 800 nm than 1466 nm photons were absorbed. We observed a ratio of unity in the insulating phase under these conditions.

The fitting of the reflectivity ratios for the insulating and metallic states (Fig. 4) produced decay constants reasonable for Auger relaxation only in the insulating state. The ratios in Fig. 4a show exponential decays of the reflectivity enhancements for the 800 nm pump over a period lasting 15 ± 3 ps (1968 nm probe) or 27 ± 4 ps and 223 ± 61 ps (1761 nm probe). The two shorter time constants may be attributable, in part, to Auger recombination (see Fig. 1d), which has been observed in other systems.[31] In contrast, the metallic ratio in Fig. 4b inset shows only a single long decay of 318 ± 60 ps, with no shorter component that would be more typically observed in Auger recombination. The longer time constants, measuring a few hundred ps, seem to correspond more closely with the lattice coming to thermal equilibrium with the photostimulated phonons.

V. PUMP WAVELENGTH AND PULSE ENERGY DENSITY DEPENDENCES

We performed additional reflectivity comparisons using the 800/1466 nm pump pair and discovered that the peak values of the 800/1466 reflectivity ratios decreased with increasing pump pulse energy density. In each comparison, the pump pulse energy densities for 800 nm and 1466 nm were the same. Figure 5 shows normalized reflectivity comparisons collected at incident pump pulse energy densities of 5.0 mJ/cm^2, 3.8 mJ/cm^2, and 2.6 mJ/cm^2. The ratios of these comparisons are shown in Fig. 6, where the ratios were fit with double exponential decays. The ratios in Figs. 6a-c near zero delay were, respectively, 1.11 ± 0.03, 1.24 ± 0.03, and 1.46 ± 0.04.

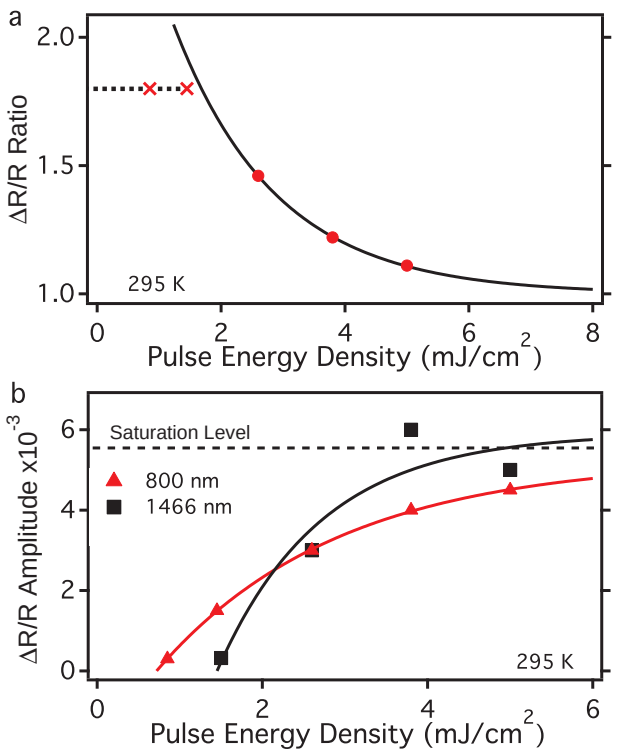

FIG. 7. (a) Pulse energy dependence of the reflectivity enhancement for 800/1466 nm pump comparisons. Filled circles (crosses) represent measurements when incident energy densities were the same (different) for both colors. (b) ΔR/R amplitudes (1761 nm probe) occurring at long delays greater than 100 ps. The saturation level was estimated as the average of the two trends. The lines in both (a) and (b) are guides for the eyes.

The faster time constants in Figs. 6a-c were 29 ps, 25 ps, and 29 ps, for an average of 28 ps. The slower time constants were 210 ps, 241 ps, and 182 ps, for an average of 211 ps. These numbers are very similar to what was observed in the data of Fig. 4a. We found the largest ratios for pump energy densities less than 2 mJ/cm^2 (Fig. 7a) while the ratio decayed toward unity as the pulse energy density increased. Figure 7b demonstrates that a long-lived (greater than 100 ps) ΔR/R component began to appear around 1 mJ/cm^2. This long-lived component in the reflectivity has been attributed to the photo-excited metallic phase,[7,11,12,14,17] therefore the decline in the reflectivity ratio correlated with the photo-excitation threshold for transiently exciting metallic clusters in the film. So, approaching unity in the ratio corresponded to approaching an incident pulse energy density capable of driving the entire probed volume transiently into the metallic phase. The threshold to the appearance of the metallic phase was also lower using the 800 nm pump (Fig. 7b).

Finally, it has been noted in prior literature[14,17] that there is a specific change that occurs in the transient reflectivity of VO_2 for a threshold pump pulse energy

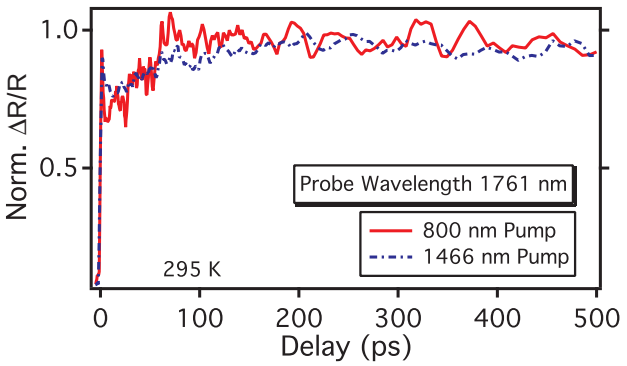

FIG. 8. Normalized transient reflectivities taken at 1.5 mJ/cm^2 for the 1466 nm pump and 0.85 mJ/cm^2 for the 800 nm pump. The data was smoothed using moving averages.

density. Below the threshold, the transient reflectivity is short-lived (less than 100 ps duration) and exhibits a typical decay response for a semiconductor. As the pump energy density rises above the threshold, the initial fast decay becomes a long-lived (greater than 1 ns) transient as a sufficient carrier density is photo-excited to initiate a longer-lived conductivity. This threshold for a long-lived transient likely corresponds to the point at which metallic clusters begin to form. We controlled the incident energy at both pump wavelengths to find where this change in the transient reflectivity occurred. In Fig. 8, this change occurred for the 1466 nm pump at an energy density of 1.5 mJ/cm^2 and at 0.85 mJ/cm^2 for the 800 nm pump. As demonstrated in Fig. 8, and similarly to Fig. 4c, the normalized transients had the same shape and there was no evidence of a difference based on the pump wavelength. This comparison makes a strong link between matching the shape of the reflectivity transients and photo-exciting similar dynamics in the film, since it was done at a specific threshold where the same process was occurring but excited by different pump colors. Figures 4c & 8 were used in Fig. 7a of the manuscript to calculate the ratios shown by the two crosses. Since these data were not collected at the same incident pump pulse energies densities, the ratio was approximated by dividing the pump pulse energy densities for the 800 nm and 1466 nm data of Figs. 4c & 8.

VI. CONCLUSION

In conclusion, the time-resolved reflectivity in a 100 nm film of VO_2 was measured for pump wavelengths which corresponded to photon energies above and below twice the gap. The normalized transients revealed an enhancement in the reflectivity ratio due to an additional carrier population appearing within the pulse overlap for the pump wavelength above the impact ionization threshold. This enhancement decayed on timescales reasonable for Auger recombination for both probe wavelengths and provided evidence for carrier multiplication via impact ionization in thin films of VO_2 as predicted previously.[4,5] Though the insulator-metal transition of VO_2 makes it unappealing for use in photovoltaic devices, this proof-of-concept study nonetheless opens a new direction of future research: it suggests that the class of strongly correlated insulators, which remain insulators under illumination, could be investigated to find those which fulfill the other requirements for efficient photovoltaic applications.

ACKNOWLEDGMENTS

S.M. acknowledges support from the NSF (DMR-1229217). S.L. and H.N.L. were supported by the U.S. Department of Energy, Office of Science, Basic Energy Sciences, Materials Sciences and Engineering Division. A portion of this work was performed at the National High Magnetic Field Laboratory, which is supported by National Science Foundation Cooperative Agreement No. DMR-1157490 and the State of Florida.

* mcgill@magnet.fsu.edu

[1] H. Takagi and H. Y. Hwang, Science **327**, 1601 (2010).
[2] J. Mannhart and D. G. Schlom, Science **327**, 1607 (2010).
[3] H. Y. Hwang, Y. Iwasa, M. Kawasaki, B. Keimer, N. Nagaosa, and Y. Tokura, Nat. Mater. **11**, 103 (2012).
[4] E. Manousakis, Phys. Rev. B **82**, 125109 (2010).
[5] J. E. Coulter, E. Manousakis, and A. Gali, Phys. Rev. B **90**, 165142 (2014).
[6] S. Biermann, A. Poteryaev, A. I. Lichtenstein, and A. Georges, Phys. Rev. Lett. **94**, 026404 (2005).
[7] A. Cavalleri, C. Tóth, C. Siders, J. Squier, F. Ráksi, P. Forget, and J. Kieffer, Phys. Rev. Lett. **87**, 237401 (2001).
[8] A. Cavalleri, H. Chong, S. Fourmaux, T. Glover, P. Heimann, J. Kieffer, B. Mun, H. Padmore, and R. Schoenlein, Phys. Rev. B **69**, 153106 (2004).
[9] A. Cavalleri, T. Dekorsy, H. Chong, J. Kieffer, and R. Schoenlein, Phys. Rev. B **70**, 161102 (2004).
[10] H.-T. Kim, Y. W. Lee, B.-J. Kim, B.-G. Chae, S. J. Yun, K.-Y. Kang, K.-J. Han, K.-J. Yee, and Y.-S. Lim, Phys. Rev. Lett. **97**, 266401 (2006).
[11] D. Hilton, R. Prasankumar, S. Fourmaux, A. Cavalleri, D. Brassard, M. El Khakani, J. Kieffer, A. Taylor, and R. Averitt, Phys. Rev. Lett. **99**, 226401 (2007).
[12] C. Kübler, H. Ehrke, R. Huber, R. Lopez, A. Halabica, R. Haglund, and A. Leitenstorfer, Phys. Rev. Lett. **99**, 116401 (2007).
[13] M. Rini, Z. Hao, R. W. Schoenlein, C. Giannetti, F. Parmigiani, S. Fourmaux, J. C. Kieffer, A. Fu-

jimori, M. Onoda, S. Wall, and A. Cavalleri, Appl. Phys. Lett. **92**, 181904 (2008).
[14] A. Pashkin, C. Kübler, H. Ehrke, R. Lopez, A. Halabica, R. F. Haglund, R. Huber, and A. Leitenstorfer, Phys. Rev. B **83**, 195120 (2011).
[15] M. Hada, K. Okimura, and J. Matsuo, Appl. Phys. Lett. **99**, 051903 (2011).
[16] C. Miller, M. Triplett, J. Lammatao, J. Suh, D. Fu, J. Wu, and D. Yu, Phys. Rev. B **85**, 085111 (2012).
[17] T. L. Cocker, L. V. Titova, S. Fourmaux, G. Holloway, H. C. Bandulet, D. Brassard, J. C. Kieffer, M. A. El Khakani, and F. A. Hegmann, Phys. Rev. B **85**, 155120 (2012).
[18] S. Wall, L. Foglia, D. Wegkamp, K. Appavoo, J. Nag, R. Haglund, J. Stähler, and M. Wolf, Phys. Rev. B **87**, 115126 (2013).
[19] H. Wen, L. Guo, E. Barnes, J. H. Lee, D. A. Walko, R. D. Schaller, J. A. Moyer, R. Misra, Y. Li, E. M. Dufresne, D. G. Schlom, V. Gopalan, and J. W. Freeland, Phys. Rev. B **88**, 165424 (2013).
[20] D. Wegkamp, M. Herzog, L. Xian, M. Gatti, P. Cudazzo, C. L. McGahan, R. E. Marvel, R. F. Haglund, A. Rubio, M. Wolf, and J. Stähler, Phys. Rev. Lett. **113**, 216401 (2014).
[21] V. R. Morrison, R. P. Chatelain, K. L. Tiwari, A. Hendaoui, A. Bruhács, M. Chaker, and B. J. Siwick, Science **346**, 445 (2014).
[22] J. Laverock, S. Kittiwatanakul, A. A. Zakharov, Y. R. Niu, B. Chen, S. A. Wolf, J. W. Lu, and K. E. Smith, Phys. Rev. Lett. **113**, 216402 (2014).
[23] K. Appavoo, B. Wang, N. F. Brady, M. Seo, J. Nag, R. P. Prasankumar, D. J. Hilton, S. T. Pantelides, and R. F. Haglund, Nano Lett. **14**, 1127 (2014).
[24] M. Bernardi, D. Vigil-Fowler, J. Lischner, J. B. Neaton, and S. G. Louie, Phys. Rev. Lett. **112**, 257402 (2014).
[25] J. E. Coulter, E. Manousakis, and A. Gali, Phys. Rev. B **88**, 041107 (2013).
[26] S. Lee, T. L. Meyer, S. Park, T. Egami, and H. N. Lee, Appl. Phys. Lett. **105**, 223515 (2014).
[27] S. Lee, I. N. Ivanov, J. K. Keum, and H. N. Lee, Scientific Reports **6**, 19621 (2016).
[28] M. Hada, K. Okimura, and J. Matsuo, Phys. Rev. B **82**, 153401 (2010).
[29] R. D. Averitt and A. J. Taylor, Journal of Physics: Condensed Matter **14**, R1357 (2002).
[30] H. W. Verleur, A. S. Barker, and C. N. Berglund, Phys. Rev. **172**, 788 (1968).
[31] R. Schaller and V. Klimov, Phys. Rev. Lett. **92**, 186601 (2004).